

Original article

3D-QSAR and docking studies of aminopyridine carboxamide inhibitors of c-Jun N-terminal kinase-1

Ping Yi ^{a,b}, Minghua Qiu ^{a,*}^a State Key Laboratory of Phytochemistry and Plant Resources in West China, Kunming Institute of Botany, Chinese Academy of Sciences, Kunming, Yunnan 650204, China^b Graduates School of the Chinese Academy of Sciences, Beijing 100039, China

Received 15 December 2006; received in revised form 11 April 2007; accepted 30 April 2007

Available online 24 May 2007

Abstract

In order to better understand the structural and chemical features of c-Jun N-terminal kinase-1 (JNK-1), which is a member of the mitogen activated protein kinase (MAP kinase) family of enzymes responsible for the serine/threonine phosphorylation of intracellular targets, 3D-QSAR studies of some aminopyridine carboxamides as c-Jun N-terminal kinase inhibitors were performed by comparative molecular field analysis (CoMFA) to rationalize the structural requirements responsible for the inhibitory activity of these compounds. The genetic algorithm of GOLD3.1 has been employed to position 54 aminopyridine carboxamides in the active sites of JNK-1 to determine the probable binding conformation. The docking results provided a reliable conformational alignment scheme for 3D-QSAR model. Based on the docking conformations, highly predictive comparative molecular field analysis (CoMFA) was performed with a cross-validated q^2 of 0.585. The non-cross-validated analysis with six optimum components revealed a conventional r^2 value of 0.988, $F = 510.200$, and an estimated standard error of 0.071. Furthermore, the CoMFA model was mapped back to the binding sites of JNK-1, to get a better understanding of vital interactions between the aminopyridine carboxamides and the kinase. Based on the docking and CoMFA analyses, we have identified some key features in the aminopyridine carboxamides that are responsible for JNK-1 inhibitory activity. The analyses may be used to design more potent aminopyridine carboxamides and predict their activity prior to synthesis.

© 2007 Elsevier Masson SAS. All rights reserved.

Keywords: 3D-QSAR; GOLD; CoMFA; c-Jun N-terminal kinase-1

1. Introduction

c-Jun N-terminal kinases (JNKs) are important cell signaling enzymes. Three distinct genes (encoded JNK-1, JNK-2 and JNK-3, respectively) have been identified and they are activated in response to various cytokines and cellular stresses such as heat shock, irradiation, hypoxia, chemotoxins and peroxides [1,2]. Among these enzymes, JNK-1 plays a central role in linking obesity and insulin resistance. JNK-1 phosphorylation of IRS-1 at Ser307 has been shown to down-regulate insulin signaling in vitro [3,4]. Conversely, absence of the JNK-1

gene protects mice from diet-induced obesity and obesity-induced insulin resistance and results in decreased adiposity and enhanced secretion of the adiponectin [5]. These results imply a role for JNK-1 in type 2 diabetes mellitus [6].

In recent years, a number of JNK inhibitors have appeared in the patent and primary literatures [7]. Especially, Szczepankiewicz, Liu and their coworkers disclosed a novel series of aminopyridine carboxamides as potent, selective, ATP-competitive pan-JNK inhibitors. The binding modes of this series of JNK inhibitors have been determined by X-ray crystallography. These crystal structures provided not only insights into the interaction mechanisms of JNKs with the inhibitors, but also valuable clues for designing new inhibitors [8–10]. In this paper, with the molecular docking and 3D-QSAR (CoMFA) analyses it is possible to get new insights into the

* Corresponding author. Tel./fax: +86 871 5223255.

E-mail address: mhchiu@mail.kib.ac.cn (M. Qiu).

relationship between the structural information of the series of 54 aminopyridine carboxamide inhibitors [10] and the inhibitory potency, aimed at identifying structural features in JNK-1 that can be used to find new inhibitors.

2. Computational details

2.1. Biological data and molecular structures

Tables 1 and 2 show a series of JNK-1 aminopyridine carboxamide inhibitors published by Gang Liu et al. in 2006 [10]; all compounds which have bioactivity described in Ref. [10] have been taken in account. All compounds were divided into a training set and a test set. Though there are many statistical tools for splitting the data set such as k-means cluster analysis [11], which was successfully performed by González and coworkers [12–14], we chose the simplest statistical strategy. Selection of the training set and test set molecules was done by considering the fact that test set molecules represent a range of biological activity and the typical chemical structures similar to those of the training set. Thus, the test set is the true representative of the training set. The structures of the training and test set molecules are given in Tables 1 and 2, respectively. Finally the training set consists of 45 compounds and the test set comprises nine compounds. The JNK-1 IC₅₀s of inhibitors were converted to pIC₅₀s ($-\log \text{IC}_{50}$ s) and used as dependent variables in the CoMFA calculations.

The 3D structures of these compounds were constructed by using molecular modeling software package Sybyl6.9 [15]. Partial atomic charges were calculated by the Gasteiger–Huckel method, and energy minimizations were performed by using the Tripos force field [16] with a distance-dependent dielectric and the Powell conjugate gradient algorithm (convergence criterion of 0.001 kcal/mol Å). Atomic coordinates for the JNK-1 complex with ligand **893** (5-cyano-*n*-(2,5-dimethoxybenzyl)-6-ethoxypyridine-2-carboxamide), used for our modeling study, have been deposited in the Brookhaven Protein DataBank [9] with a resolution of 3.0 Å (PDB ID:2H96).

2.2. Docking studies

To locate the appropriate binding orientations and conformations of these aminopyridine carboxamide inhibitors interacting with JNK-1, a powerful computational searching method is needed. The advanced molecular docking program GOLD, version 3.1 [17], which uses a powerful genetic algorithm (GA) method for conformational search and docking programs, was employed to generate an ensemble of docked conformations. The structures of JNK-1 and aminopyridine carboxamide inhibitors were built by using the Sybyl6.9 molecular modeling software. The original ligand was removed from the coordinated set. The genetic operators were 100 for the population size, 1.1 for the selection, 5 for the number of subpopulations, 100,000 for the maximum number of genetic applications, and 2 for the size of the niche used to increase population diversity. The weights were chosen so that

crossover mutations were applied with equal probability (95/95 for the values) and migration was applied 5% of the time.

2.3. Choice of docking fitness functions

ChemScoring function encoded in GOLD was applied to predict binding positions between JNK-1 and 54 inhibitors. This scoring function was described by Eldridge et al. [18,19]. The fitness score is taken as the negative of the sum of the component energy terms, so that larger fitness scores are better [20].

2.4. Structural alignment

Ten conformations were obtained though GOLD for each ligand and all conformations were extracted from the optimized inhibitor–JNK-1 complex. After superimposing the aminopyridine fragments of these conformations, the conformations with the highest ChemScores for each ligand of the training set were aligned together inside the binding pocket of JNK-1 and used directly for CoMFA to explore the specific contributions of electrostatic and steric effects of the molecular bioactivities. The conformations for each ligand of the test set were chosen to have lowest residues between actual and predicted pIC₅₀, which was predicted by the CoMFA model of the training set.

2.5. CoMFA

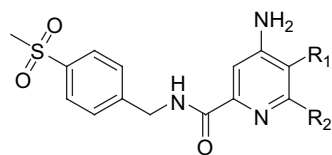
Steric and electrostatic interactions were calculated using the Tripos force field with a distance-dependent dielectric constant at all intersections in a regular space (2 Å) grid taking a sp³ carbon atom as steric probe and +1 charge as electrostatic probe. The cutoff was set to 30 kcal/mol. With standard options for scaling of variables, the regression analysis was carried out using the full cross-validated partial least-squares (PLS) methods of leave-one-out (LOO). The minimum-sigma (column filtering) was set to 2.0 kcal/mol to improve the signal-to-noise ratio by omitting those lattice points whose energy variation was below this threshold. The final model, noncross-validated conventional analysis, was developed with the optimum number of components to yield a noncross-validated r^2 value.

3. Results and discussion

3.1. Binding conformations of aminopyridine carboxamides

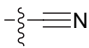
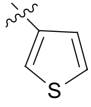
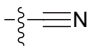
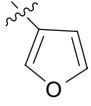
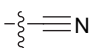
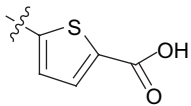
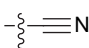
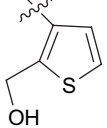
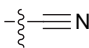
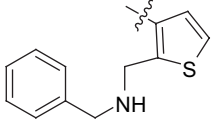
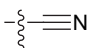
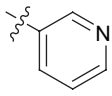
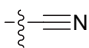
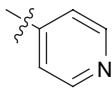
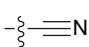
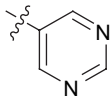
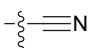
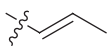
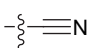
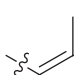
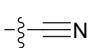
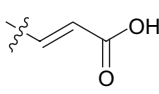
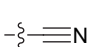
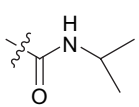
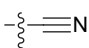
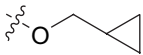
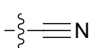
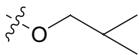
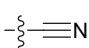
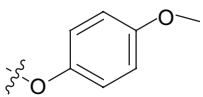
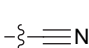
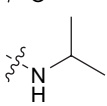
In order to determine the probable binding conformations of these aminopyridine carboxamides, the GOLD was used to dock all compounds into the active sites of JNK-1. The docking reliability was validated using the known X-ray structure of JNK-1 in complex with the molecular ligand **893** (5-cyano-*n*-(2,5-dimethoxybenzyl)-6-ethoxypyridine-2-carboxamide). The ligand **893** was redocked to the binding sites of JNK-1 and the docked conformation corresponding to the

Table 1

Structures, experimental activities (pIC₅₀s), predicted activities (PAs), residuals by CoMFA model, and docking ChemScores in the training set

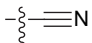
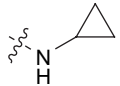
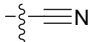
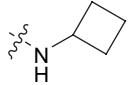
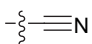
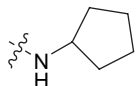
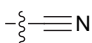
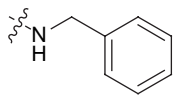
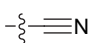
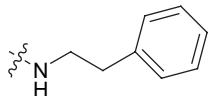
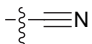
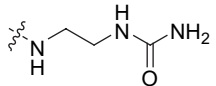
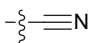
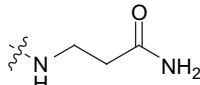
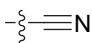
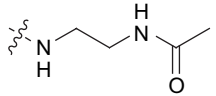
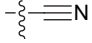
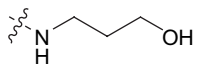
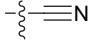
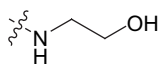
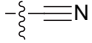
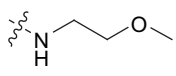
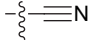
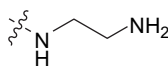
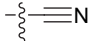
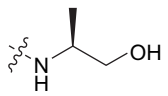
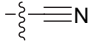
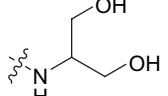
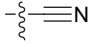
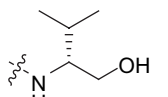
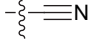
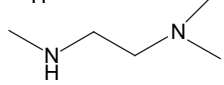
Compound	R1	R2	pIC ₅₀	Predict	Residue	ChemScore
1			6.456	6.495	0.039	21.22
2			5.465	5.525	−0.060	22.53
3			5.963	5.991	−0.028	17.88
4			5.650	5.564	0.086	17.53
5			5.810	5.780	0.030	17.91
6			5.928	5.854	0.074	17.90
7			5.533	5.508	0.025	21.04
8			7.102	7.010	0.092	19.64
9			6.498	6.452	0.046	16.92
10			5.280	5.353	−0.073	17.90
11			6.699	6.698	0.001	25.68
12			6.367	6.403	−0.036	25.18
13			7.367	7.341	0.026	24.61

Table 1 (continued)

Compound	R1	R2	pIC ₅₀	Predict	Residue	ChemScore
14			7.092	7.070	0.022	23.74
15			6.569	6.827	−0.258	22.45
16			6.602	6.704	−0.102	23.63
17			6.244	6.161	0.083	25.50
18			5.701	5.715	−0.014	26.81
19			6.495	6.482	0.013	23.66
20			6.276	6.204	0.072	23.70
21			6.208	6.203	0.005	21.25
22			7.319	7.253	0.066	22.68
23			6.824	6.900	−0.076	22.39
24			6.523	6.515	0.008	25.09
25			6.367	6.335	0.032	20.24
26			7.638	7.590	0.048	19.73
27			7.056	7.135	−0.079	20.38
28			6.377	6.371	0.006	19.65
29			7.174	7.252	−0.078	20.73

(continued on next page)

Table 1 (continued)

Compound	R1	R2	pIC ₅₀	Predict	Residue	ChemScore
30			7.495	7.440	0.055	21.62
31			7.071	7.147	−0.076	22.44
32			7.018	7.041	−0.023	21.20
33			6.086	6.109	−0.023	24.21
34			6.585	6.591	−0.006	25.14
35			7.032	7.020	0.012	22.19
36			7.180	7.185	−0.005	21.76
37			7.229	7.270	−0.041	23.06
38			7.268	7.240	0.028	22.48
39			7.032	6.916	0.116	22.50
40			6.921	6.878	0.043	21.25
41			5.796	5.789	0.007	23.86
42			6.745	6.725	0.020	21.34
43			7.119	7.060	0.059	22.08
44			5.824	5.884	−0.060	23.19
45			5.137			22.65

highest ChemScore was selected as the most probable binding conformation. The root-mean-square deviation (RMSD) between the conformations of **893** and docked **893** is equal to 0.54 Å, suggesting that a high docking reliability of GOLD in reproducing the experimentally observed binding mode of JNK-1 inhibitors and the parameter set of the GOLD simulation is reasonable to reproduce the X-ray structure. Because the **893** is the same type structure as the aminopyridine carboxamides which are shown in Tables 1 and 2, the GOLD method and the parameter set could be extended to search the JNK-1 binding conformations for other inhibitors accordingly.

Fig. 1 shows the 3D model of aminopyridine carboxamides at the active sites of JNK-1 and Fig. 2 illustrates the probable binding conformational alignment for the 54 aminopyridine carboxamides chosen from the docked conformations. All of the aminopyridine carboxamide inhibitors are bonded in the active sites of JNK-1 in a similar conformation of **893** (Fig. 1), and the common chain structures superimposed

each other well. Based on this set of binding conformations and their alignment, after superimposing the aminopyridine fragments of these inhibitors, CoMFA was performed.

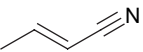
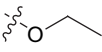
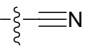
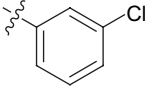
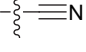
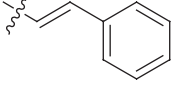
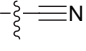
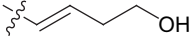
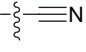
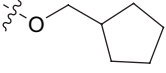
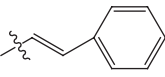
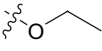
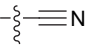
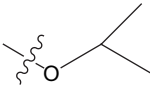
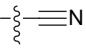

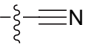
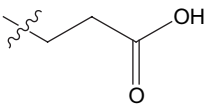
3.2. Docking study

All 54 inhibitors have been docked in the binding pocket of JNK-1 by using GOLD. Orientations of 54 docking solutions were selected to perform CoMFA study, and the ChemScores of these inhibitors are shown in Tables 1 and 2.

In addition, Fig. 3(a) and (b) represents the interaction model of the docked inhibitor **34** with JNK-1. Inhibitor **34** binds to the active site and makes several interactions with the hinge-binding region of the enzyme. As shown in Fig. 3b, inhibitor **34** form two hydrogen bonds with Glu109 and Met111. The pyridine ring in **34** interacts with the hydrophobic surface of the side chains of Ile32, Val40, Ala53, Ile86, Val158 and Leu168. The *p*-methanesulfonylbenzyl fragment in **34** twisting outside the active cave interacts with the

Table 2

Structures, experimental activities (pIC₅₀s), predicted activities (PAs), residuals by CoMFA model, and docking ChemScores in the test set

Compound	R1	R2	pIC ₅₀	Predict	Residue	ChemScore
46			6.387	6.993	−0.606	17.85
47			5.928	6.618	−0.690	23.55
48			5.839	6.538	−0.699	27.96
49			6.770	7.152	−0.382	23.24
50			6.409	6.706	−0.297	20.72
51			5.614	5.631	−0.017	22.65
52			7.824	6.960	0.864	18.10
53			7.658	7.010	0.648	20.17
54			5.785	6.249	−0.464	21.85

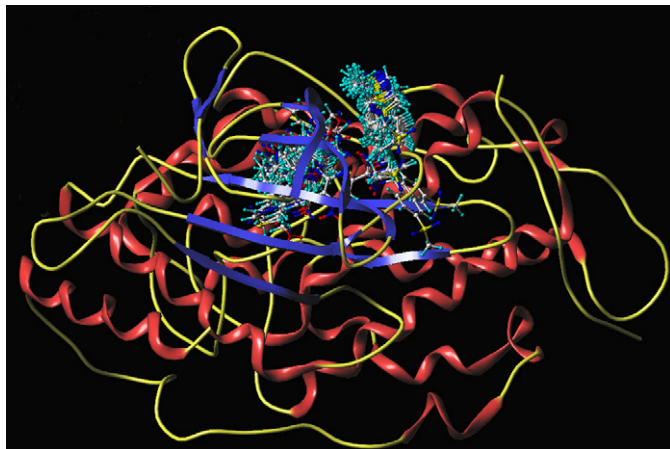


Fig. 1. Binding conformations of docked compounds at the active sites of JNK-1.

hydrophobic surface of the side chains of Ile32 and Ala42. The phenethyl amine fragment in **34** is surrounded not only by the hydrophobic side chains of Gly35, Gly38 and Ile39, but also by the polar side chains of Ser34, Lys55, Ser155, Asn156 and Asp169. A further examination of the structural complex also reveals that the 5-cyano group in **34** is pointed toward the residue Met108. It is known that this residue can act as a gate-keeper and controls kinase selectivity of a wide range of structurally unrelated compounds [21].

3.3. CoMFA model

After omitting the compound **45**, 44 JNK-1 inhibitors were picked up as training set for constructing CoMFA model, the remaining nine used as test set for the model validation. PLS analysis was carried out for the 53 binding conformations, and the results are listed in Table 3, which showed that a CoMFA model with a cross-validated q^2 of 0.585 for

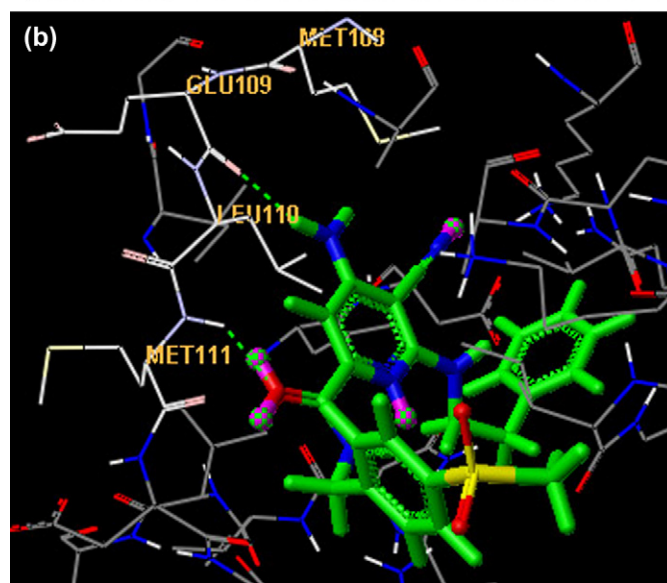
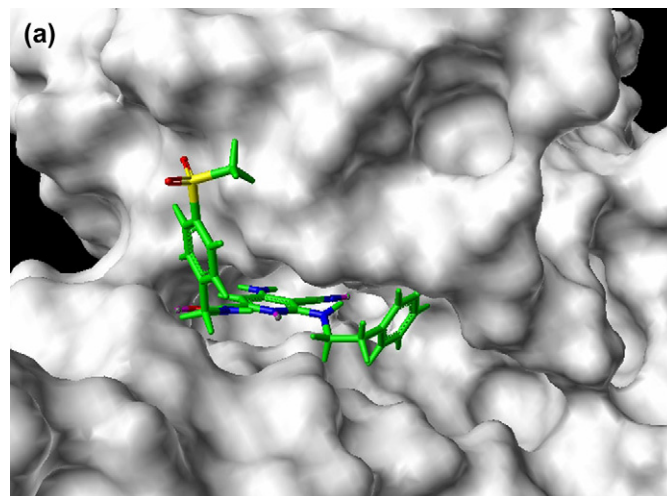


Fig. 3. (a) Inhibitor **34** docked in the binding pocket of JNK-1 using GLOD. (b) Two H-bonds (as highlighted by the dashed lines in green color) between compound **34** and JNK-1. (For interpretation of the references to color in the figure legends, the reader is referred to the web version of this article.)

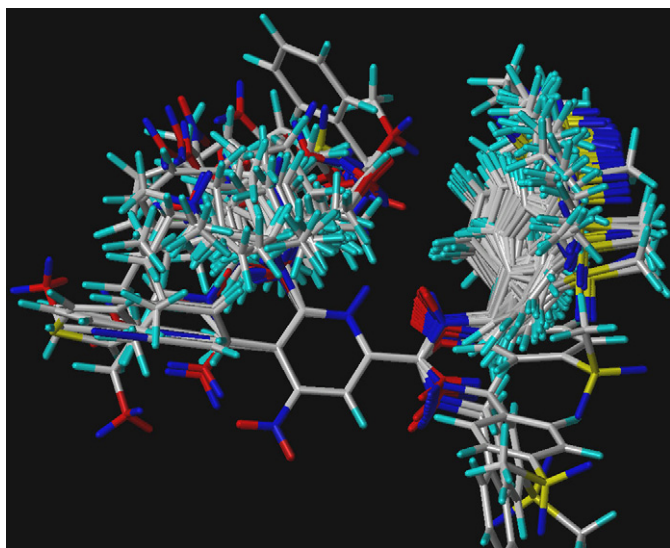


Fig. 2. Superimposition of 54 aminopyridine carboxamides for 3D-QSAR studies.

six components was obtained. In addition, cross-validated PLS analyses have been carried out with the components from 1 to 7, respectively. The results revealed with six components the lowest standard error of predictions value of 0.421 was obtained. The cross-validated q^2 of 0.592 for seven components is little higher than the cross-validated q^2 of 0.585 for six components, however, in practice, models with fewer components are more robust, finally six components were adopted as the optimum components for the training set. The noncross-validated PLS analysis with six components revealed a conventional r^2 value of 0.988, $F = 510.200$, and an estimated standard error of 0.071. The steric field descriptors explain 54.3% of the variance, while the electrostatic descriptors explain 45.7%. The predicted activities for the 44 inhibitors versus their experimental activities with their residues are listed in Table 1. The correlation between the predicted activities and the experimental activities is depicted in Fig. 4. Table 1

Table 3
Summary of CoMFA analysis

Parameter	CoMFA
PLS statistics	
Leave-one-out (LOO)	
q^2 (CV correlation coefficient)	0.585
N (number of components)	6
SEP (standard error of prediction)	0.421
Un-cross-validated	
r^2 (correlation coefficient)	0.988
SEE (standard error of estimate)	0.071
F (F -ratio)	510.2
Field distribution (%)	
Steric	54.3
Electrostatic	45.7
Testing set	
r^2 (correlation coefficient)	0.902
S (standard error of prediction)	0.215

and Fig. 4 demonstrate that the predicted activities by the constructed CoMFA model are in good agreement with the experimental data, suggesting that a reliable CoMFA model was successfully constructed.

The CoMFA result is usually represented as 3D ‘coefficient contour’. It shows regions where variations of steric and electrostatic nature in the structural features of the different molecules contained in the training set lead to increase or decrease in the activity. The CoMFA steric and electrostatic fields are presented as contour plots in Fig. 6. To aid in visualization, compound **34** is displayed in the map as a reference structure. Green-colored¹ regions indicate areas where increased steric bulk is associated with enhanced JNK-1 inhibitory activity, and yellow regions suggest areas where increased steric bulk is unfavorable to activity. Blue-colored regions show areas where more positively charged groups are favorable to JNK-1 inhibitory activity. While red regions represent areas where increased negatively charged groups are favorable to activity.

To get a better understanding of relationship between the binding pocket of JNK-1 and the contours of CoMFA, the binding pocket graph in Fig. 5 represents interactions between the binding pocket proteins and docked compound **34**. The compound **34** in Fig. 5 is the same pose as shown in Fig. 6.

The steric contour of CoMFA (Fig. 6a) shows a big green contour just above the *p*-methanesulfonylbenzyl group in compound **34**, for the link group between the *p*-methanesulfonylbenzyl and aminopyridine is CH₂ which is flexible, the *p*-methanesulfonylbenzyl group in different inhibitors may twist up and down respectively just as shown in Fig. 2 when they docked in the JNK-1 pocket. The upper *p*-methanesulfonylbenzyl groups which twist outside the pocket may have hydrophobic interactions with the side chains of Ile32 and Ala42; it is not strange that there is a big green contour just above the *p*-methanesulfonylbenzyl group in compound **34**. However,

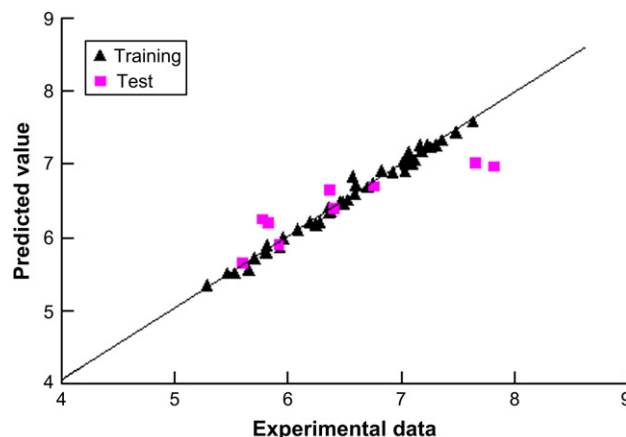


Fig. 4. Correlation between predicted activities (PA) by CoMFA models and the experimental pIC₅₀ values of training and test sets. (Black filled triangles represent predictions for the training set, while pink filled rectangles represent predictions for the test sets.)

the lower *p*-methanesulfonylbenzyl group may be blocked by Asp112 and Ala133, so there are several yellow contours in the upper right corner of Fig. 6a. Because the residue Asp112 is polar negative charged amino acid, it is reasonable that three red contours are shown in the middle right corner of Fig. 6b.

In the left bottom corner of Fig. 6a, there is a big yellow contour, where at the same position of JNK-1 the residues Met108, Lys55, Ile106, Met77 and Glu73 are located, which are pre-characterized as a wall. That is why compound **18** showed lower activity than the most of other inhibitors for it has a big R₂ substituent. The green belt contours shown in the middle bottom of Fig. 6a represent that there are favorable regions for steric

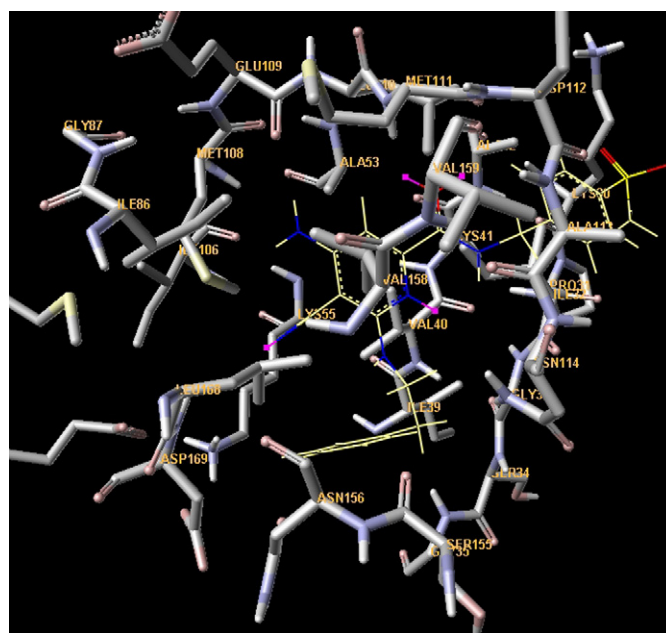


Fig. 5. The interactions between the binding pocket proteins and docked yellow-colored compound **34**.

¹ For interpretation of the references to color in the text, the reader is referred to the web version of this article.

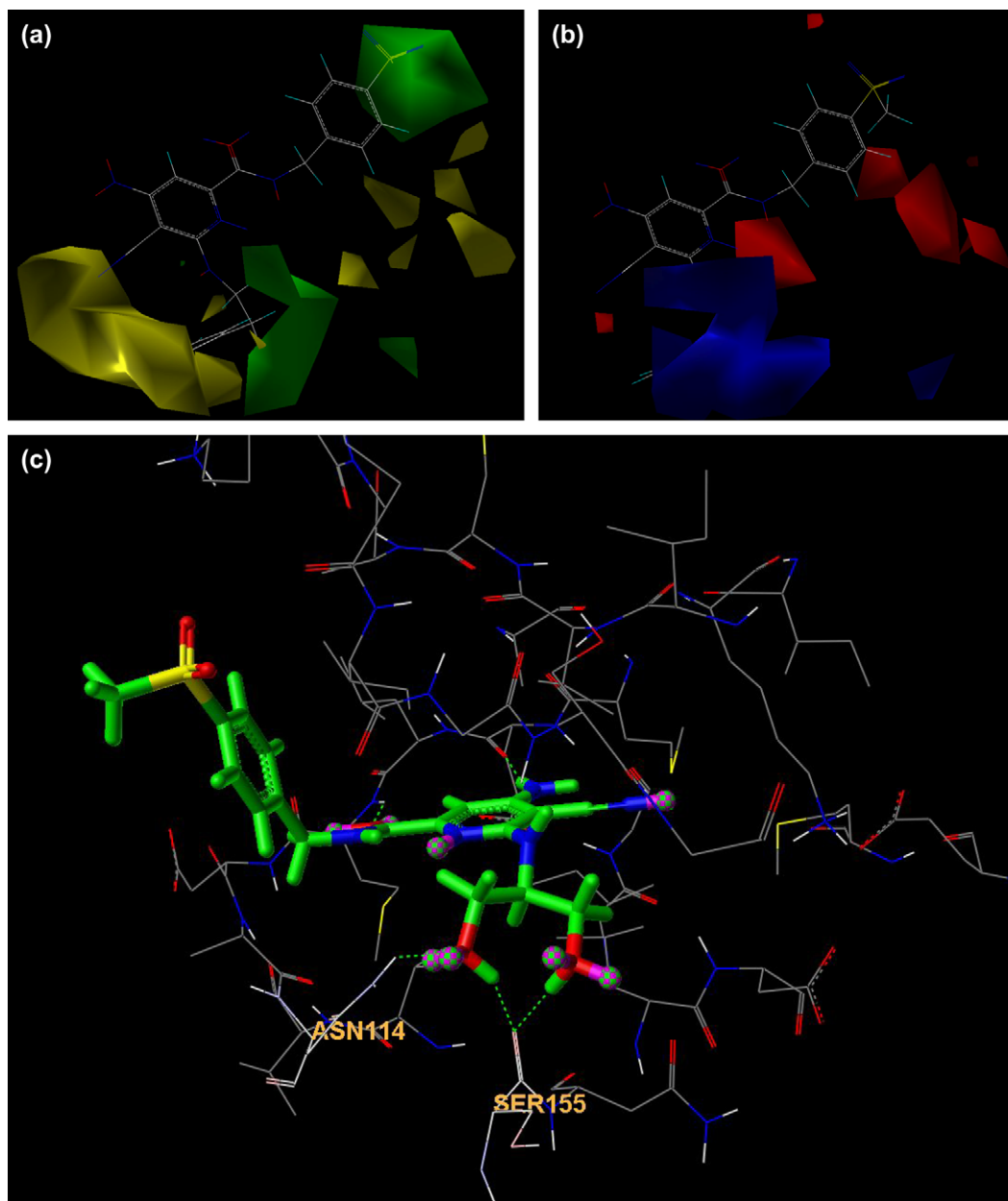


Fig. 6. CoMFA contour maps in combination with inhibitor **34**. (a) The steric field distribution. (b) The electrostatic field distribution. Sterically favored areas are in green; sterically unfavored areas are in yellow. Positive potential favored areas are in blue; positive potential unfavored areas are in red. (c). Three H-bonds between (as highlighted by the dashed lines in green color) R_2 substituent of compound **43** and JNK-1.

interaction. The nearest pocket residues are Val40, Lys55 and Leu168 which all have hydrophobic side chains. Small hydrophobic R_2 substituents may have hydrophobic interaction with the side chains of Val40, Lys55 and Leu168 well. It is one reason why compounds **22**, **23**, **26**, **27**, **29**, **30**, **31** and **32** have high bio-activities, for they all have small hydrophobic R_2 substituents. If the chains of R_2 substituents are longer, they may interact with the pocket gate residues Ser155, Asn156, Asn114, Gly33, Ser34, and Gly35 which are all polar uncharged amino acids; more positive charged R_2 substituents of the inhibitors at this region may interact well with the oxygen atom in the side chain of these amino acid residues. It is reasonable that at the almost same region there is a big blue belt shown in Fig. 6b. The

information given above indicated that polar electrophilic R_2 substituents might have higher activity. As we all know, the hydrogen in the NH or OH group is electrophilic, further docking study showed that the carbonyl, NH or OH group on the R_2 substituents in compounds **35**, **36**, **37**, **38**, **39** and **43** might form H-bonds with one or two residues of Ser34, Gly35, Asn114 and Ser155. Moreover, the R_2 substituents containing carbonyl, NH or OH group might also have strong electrostatic interactions with the residues Ser34, Gly35, Asn114, Ser155 and Asn156. That is the reason why compounds **35**, **36**, **37**, **38**, **39** and **43** have higher activity than most of other inhibitors. Fig. 6c shows that the R_2 substituent in compound **43** formed three H-bonds with the residues Asn114 and Ser155. Docking

study also showed that the R_2 substituents in compounds **41**, **42**, **43** and **45** did not form H-bonds with JNK-1 and were far away from the residues Ser34, Gly35, Asn114 and Ser155. Maybe that is one reason why compounds **41**, **42**, **43** and **45** have lower activities than compounds **35**, **36**, **37**, **38**, **39** and **43**. Additionally, there is a small red unfavorable negative charges contour showed in the left bottom corner of Fig. 6b and at the same position of the active pocket is the residue Met108; it is known that the sulfur of Met is a good nucleophile, so the negative charged R_1 substituents may not interact well with the sulfur of Met108. This can explain why compounds **1** and **9** have more activity than compounds **2–8**. At last there was a red contour in the center of Fig. 6b, the carbonyl group on the backbone of Ile32 is at the center of the red contour, pointing towards the pyridine of the inhibitors. More negative charged R_2 substituents appear at this region may not interact well with the carbonyl group of Ile32.

3.4. Validation of the 3D-QSAR models

The nine randomly selected compounds (Table 2) were used as the test set to verify the constructed CoMFA models. The calculated results are listed in Table 2 and displayed in Fig. 4 (pink rectangle). The predicted pIC_{50} with the QSAR models are in good agreement with the experimental data with a statistically tolerable error range and with a correlation coefficient of $r^2 = 0.902$ (Table 3). The test results indicated that the CoMFA model would be reliably used in new inhibitor design for developing drug against type 2 diabetes mellitus.

4. Conclusion

In this study, using the alignment scheme generated from the docking study, a highly predictive CoMFA model was developed on aminopyridine carboxamide JNK-1 inhibitors. The satisfactory model was obtained with leave-one-out (LOO) cross-validation q^2 and conventional r^2 values of 0.585 and 0.988, respectively. The binding conformations of 54 aminopyridine carboxamides were determined and predicted by molecular docking. The reliability of the model was verified by the compounds in the test set. The consistency between the CoMFA field distributions and the 3D topology of the protein structure showed the robustness of 3D-QSAR model. Moreover, the docking/3D-QSAR results suggested that aminopyridine carboxamides form two hydrogen bonds to the backbones of amino acids Glu109 and Met111 as the ‘classical’ hinge interactions. A inhibitor which contains small less negative charges R_1 substituent and a R_2 substituent which is small hydrophobic or intend to form H-bonds with JNK-1 may have high bioactivity. These results demonstrated the power of combining docking/QSAR approach to explore the probable binding conformations of compounds at the active sites of the protein target, and further provided useful

information to understand the structural and chemical features of JNK-1 in designing and finding new potential inhibitors.

Acknowledgements

The authors are grateful to the State Key Laboratory of Phytochemistry and Plant Resources in West China and Xibuzhiguang program of CAS for financial support.

References

- [1] J.M. Kyriakis, J. Avruch, *Physiol. Rev.* 81 (2001) 807–869.
- [2] G. Pearson, R. Robinson, T.B. Gibson, B.-E. Xu, M. Karandikar, K. Berman, M.H. Cobb, *Endocr. Rev.* 22 (2001) 153–183.
- [3] V. Aguirre, T. Uchida, L. Yenush, R.J. Davis, M.F. White, *J. Biol. Chem.* 275 (2000) 9047–9054.
- [4] V. Aguirre, E.D. Werner, J. Giraud, Y. Lee, S.E. Shoelson, *J. Biol. Chem.* 277 (2002) 1531–1537.
- [5] J. Hirosumi, G. Tuncman, L. Chang, C.Z. Görgün, K. Teoman Uysal, K. Maeda, M. Karin, G.S. Hotamisligil, *Nature* 420 (2002) 333–336.
- [6] B.L. Bennet, Y. Satoh, A.J. Lewis, *Curr. Opin. Pharmacol.* 3 (2003) 420–425.
- [7] G. Liu, C.M. Rondinone, *Curr. Opin. Investig. Drugs* 6 (2005) 979–987.
- [8] B.G. Szczepankiewicz, C. Kosogof, L.T.J. Nelson, G. Liu, B. Liu, H. Zhao, M.D. Serby, Z. Xin, M. Liu, R.J. Gum, D.L. Haasch, S. Wang, J.E. Clampit, E.F. Johnson, T.H. Lubben, M.A. Stashko, E.T. Olejniczak, C. Sun, S.A. Dorwin, K. Haskins, C. Abad-Zapatero, E.H. Fry, C.W. Hutchins, H.L. Sham, C.M. Rondinone, J.M. Trevillyan, *J. Med. Chem.* 49 (2006) 3563–3580.
- [9] H. Zhao, M.D. Serby, Z. Xin, B.G. Szczepankiewicz, M. Liu, C. Abad-Zapatero, E.H. Fry, E.F. Johnson, S. Wang, T. Pederson, R.J. Gum, D.E. Haasch, J.E. Clampit, C. Rondinone, J.M. Trevillyan, H.L. Sham, G. Liu, *J. Med. Chem.* 49 (2006) 4455–4458.
- [10] G. Liu, H.Y. Zhao, B. Liu, Z.L. Xin, M. Liu, C. Kosogof, B.G. Szczepankiewicz, S.Y. Wang, J.E. Clampit, R.J. Gum, D.L. Haasch, J.M. Trevillyan, H.L. Sham, *Bioorg. Med. Chem.* 16 (2006) 5723–5730.
- [11] R.B. Kowalski, S. Wold, in: P.R. Krishnaiah, L.N. Kanal (Eds.), *Pattern Recognition in Chemistry*, In Handbook of Statistics, North Holland Publishing Company, Amsterdam, 1982, pp. 673–697.
- [12] M.P. González, A.M. Helguera, M.A. Cabrera, *Bioorg. Med. Chem.* 13 (2005) 1775–1781.
- [13] M.P. González, L.C. Dias, A.M. Helguera, Y.M. Rodriguez, L.G. de Oliveira, L.T. Gomez, H.G. Diaz, *Bioorg. Med. Chem.* 12 (2004) 4467–4475.
- [14] E. Molina, H.G. Diaz, M.P. González, E. Rodriguez, E. Uriarte, *J. Chem. Inf. Comput. Sci.* 44 (2004) 515–521.
- [15] Sybyl Version 6.9, Tripos Associates, St. Louis, MO, 2001.
- [16] M. Clark, R.D. Cramer, N.V. Opdenbosch, *J. Comput. Chem.* 10 (1989) 982–1012.
- [17] G. Jones, P. Willett, R.C. Glen, A.R. Leach, R. Taylor, *J. Mol. Biol.* 267 (1997) 727–748.
- [18] M.D. Eldridge, C.W. Murray, T.R. Auton, G.V. Paolini, R.P. Mee, *J. Comput. Aided Mol. Des.* 11 (1997) 425–445.
- [19] C.A. Baxter, C.W. Murray, D.E. Clark, D.R. Westhead, M.D. Eldridge, *Proteins* 33 (1998) 367–382.
- [20] M.L. Verdonk, J.C. Cole, M.J. Hartshorn, C.W. Murray, R.D. Taylor, *Proteins* 52 (2003) 609–623.
- [21] S. Blencke, B. Zech, O. Engkvist, Z. Greff, L. Orfi, Z. Horvath, G. Keri, A. Ullrich, H. Daub, *Chem. Biol.* 11 (2004) 691–701.